J. Fluid Mech. (1994), *vol.* 272, *pp.* 135–156

Different forms for nonlinear standing waves in deep water

By PETER J. BRYANT[1] AND MICHAEL STIASSNIE[2]

[1] Department of Mathematics, University of Canterbury, Christchurch, New Zealand

[2] Department of Civil Engineering, Technion-Israel Institute of Technology, Haifa, Israel.

(Received 29 August 1993 and in revised form 24 January 1994)

Multiple forms for standing waves in deep water periodic in both space and time are obtained analytically as solutions of Zakharov's equation and its modification, and investigated computationally as irrotational two-dimensional solutions of the full nonlinear boundary value problem. The different forms are based on weak nonlinear interactions between the fundamental harmonic and the resonating harmonics of 2, 3, ... times the frequency and 4, 9, ... respectively times the wavenumber. The new forms of standing waves have amplitudes with local maxima at the resonating harmonics, unlike the classical (Stokes) standing wave which is dominated by the fundamental harmonic. The stability of the new standing waves is investigated for small to moderate wave energies by numerical computation of their evolution, starting from the standing wave solution whose only initial disturbance is the numerical error. The instability of the Stokes standing wave to sideband disturbances is demonstrated first, by showing the evolution into cyclic recurrence that occurs when a set of nine equal Stokes standing waves is perturbed by a standing wave of a length equal to the total length of the nine waves. The cyclic recurrence is similar to that observed in the well-known linear instability and sideband modulation of Stokes progressive waves, and is also similar to that resulting from the evolution of the new standing waves in which the first and ninth harmonics are dominant. The new standing waves are only marginally unstable at small to moderate wave energies, with harmonics which remain near their initial amplitudes and phases for typically 100–1000 wave periods before evolving into slowly modulated oscillations or diverging.

1. Introduction

Standing waves may be generated at the free surface of deep water contained between two parallel vertical walls. The most important feature is that their spectrum with respect to the coordinate perpendicular to the walls is discrete, with wavenumbers which are integral multiples of π/l, where l is the distance between the walls. If they are also periodic in time we describe them as *pure standing waves*, in contrast to standing waves which are evolving in time.

Although Stokes investigated nonlinear progressive waves in the middle of last century, it appears that it was not until Rayleigh (1915) presented the third-order theory that investigations of nonlinear standing waves at the free surface of deep water have been reported. Penney & Price (1952) extended Rayleigh's method to the fifth order and applied it to a postulate that the stable standing wave of greatest height has a crest of right-angled nodal form. Taylor (1953) tested the results of Penney & Price experimentally, showing reasonable agreement with their conclusions although he disagreed with parts of their arguments. Saffman & Yuen (1979) used a numerical

scheme which calculates the evolving position of the free surface to obtain wave profiles consistent with those predicted by Penney & Price and observed by Taylor. It is noted that the standing waves observed by Taylor and calculated by Saffman & Yuen are not pure standing waves. The different forms of standing waves described in the present investigation are pure standing waves, although in addition we do calculate their time evolution properties.

Schwarz & Whitney (1981) and Rottman (1982) developed high-order expansions which were summed with the assistance of Padé approximants, with the aim in both investigations of understanding the approach to the wave of greatest height. The present investigation is restricted to standing waves of small to moderate heights. Mercer & Roberts (1992) also studied steep standing waves using a distribution of vortices on the water surface, in a semi-Lagrangian approach. All of the above authors restricted themselves to pure standing waves with a *Stokes ordering of harmonic amplitudes*. Rottman (1982), however, indicated the possibility of different solutions with a different ordering of harmonic amplitudes, but did not pursue it in detail.

Glozman, Agnon & Stiassnie (1993) and Agnon *et al.* (1992) derived and used a recursive high-order Hamiltonian formulation of the water wave problem to study standing waves. Glozman *et al.* focused their computation on the interaction of the fundamental harmonic with the fourth harmonic in pure standing waves. They found, in addition to the Stokes type of wave, four new waves in which the fourth harmonic is comparable to the fundamental harmonic. Agnon *et al.* investigated all five waves (which they denoted S, A, B, C and D) using 12 to 20 harmonics, and found that all exist to high order.

In the present investigation, we study the existence, stability, and long-time behaviour of these and other new standing waves. There is no formal proof of existence yet, even for the Stokes type of standing wave S. Amick & Toland (1987) addressed the existence problem for the Stokes type but stated that the analytical question of the convergence of the relevant series remains open.

Okamura (1984) used Zakharov's equation, which is correct to the third order, to make calculations of the linear stability of the Stokes type of standing waves. The regions of instability of these waves to two- and three-dimensional standing wave disturbances were found. Although the mathematical description is consistent and the calculations at the lower wave steepnesses appear to be correct, there is a degree of abstraction in allowing the standing wave disturbances to have a continuous spectrum, unrelated to the discrete spectrum of the standing waves themselves. Also, the third-order theory is not valid at the higher wave steepnesses considered. Stiassnie & Shemer (1984) modified Zakharov's equation in extending it to the fourth order. We use their improved formulation to find the regions of linear instability applicable to the different standing waves considered below.

2. Theory

2.1. *Background*

The equations governing the irrotational motion of waves on the free surface of deep water are

$$\nabla^2\phi = 0, \quad z \leqslant \eta(x,t), \tag{2.1a}$$

$$\left.\begin{aligned} \eta_t + \nabla\phi\cdot\nabla\eta - \phi_z &= 0 \\ \phi_t + \tfrac{1}{2}(\nabla\phi)^2 + gz &= 0 \end{aligned}\right\}, \quad z = \eta(x,t), \tag{2.1b}$$

$$|\nabla\phi| \to 0, \quad z \to -\infty, \tag{2.1c}$$

where $\phi(\boldsymbol{x}, z, t)$ is the velocity potential, $\eta(\boldsymbol{x}, t)$ is the displacement of the free surface and g the gravitational acceleration. The horizontal coordinates are $\boldsymbol{x} = (x, y)$, the vertical coordinate z is pointing upwards, and t is time.

When initial conditions are given in terms of $\eta(\boldsymbol{x}, 0), \phi(\boldsymbol{x}, \eta(\boldsymbol{x}, 0), 0)$, the problem can be transformed into an evolution equation in the Fourier plane

$$\mathrm{i}\frac{\partial B}{\partial t} = I_3(\boldsymbol{k}, t) + I_4(\boldsymbol{k}, t) + I_5(\boldsymbol{k}, t) + \ldots. \tag{2.2}$$

The new dependent variable $B(\boldsymbol{k}, t)$ is a *free component* of the wave field (as distinct from the bound components defined below), and $I_3, I_4, I_5, \ldots$, are integral operators representing quartet, quintet, sextet, ..., nonlinear interactions respectively.

The leading term I_3 on the right-hand side of (2.2) was first derived by Zakharov (1968), and the higher-order term I_4 by Stiassnie & Shemer (1984):

$$I_3 = \int\int\int_{-\infty}^{\infty} T^{(2)}_{0,1,2,3}\, B_1^* B_2 B_3\, \delta(\boldsymbol{k}+\boldsymbol{k}_1-\boldsymbol{k}_2-\boldsymbol{k}_3)\, \mathrm{e}^{\mathrm{i}(\omega+\omega_1-\omega_2-\omega_3)t}\, \mathrm{d}\boldsymbol{k}_1\, \mathrm{d}\boldsymbol{k}_2\, \mathrm{d}\boldsymbol{k}_3, \tag{2.3a}$$

$$\begin{aligned} I_4 = \int\int\int\int_{-\infty}^{\infty} \{ & U^{(2)}_{0,1,2,3,4}\, B_1^* B_2 B_3 B_4\, \delta(\boldsymbol{k}+\boldsymbol{k}_1-\boldsymbol{k}_2-\boldsymbol{k}_3-\boldsymbol{k}_4) \\ & \times \mathrm{e}^{\mathrm{i}(\omega+\omega_1-\omega_2-\omega_3-\omega_4)t} + U^{(3)}_{0,1,2,3,4}\, B_1^* B_2^* B_3 B_4\, \delta(\boldsymbol{k}+\boldsymbol{k}_1+\boldsymbol{k}_2-\boldsymbol{k}_3-\boldsymbol{k}_4) \\ & \times \mathrm{e}^{\mathrm{i}(\omega+\omega_1+\omega_2-\omega_3-\omega_4)t} \}\, \mathrm{d}\boldsymbol{k}_1\, \mathrm{d}\boldsymbol{k}_2\, \mathrm{d}\boldsymbol{k}_3\, \mathrm{d}\boldsymbol{k}_4, \end{aligned} \tag{2.3b}$$

where a compact notation is used in which the arguments $\boldsymbol{k}_i$ are replaced by the subscript i and the subscript zero is assigned to $\boldsymbol{k}$. The Dirac delta function of the two-dimensional vector $\boldsymbol{k}$ is defined as

$$\delta(\boldsymbol{k}) = \frac{1}{(2\pi)^2}\int_{-\infty}^{\infty} \mathrm{e}^{\mathrm{i}\boldsymbol{k}\cdot\boldsymbol{x}}\, \mathrm{d}\boldsymbol{x}. \tag{2.3c}$$

The frequency ω is related to $\boldsymbol{k}$ through the linear dispersion relation $\omega(\boldsymbol{k}) = (g|\boldsymbol{k}|)^{\frac{1}{2}}$. The kernels $T^{(2)}_{0,1,2,3}, U^{(2)}_{0,1,2,3,4}, \ldots$, as well as other kernels to appear subsequently, are given in Stiassnie & Shemer (1984). The asterisk denotes the complex conjugate. The component $B(\boldsymbol{k}, t)$ is related to the Fourier transform (denoted by $\hat{}$) of $\eta(\boldsymbol{x}, t)$ and of the velocity potential at the free surface, $\phi^s(\boldsymbol{x}, t) = \phi(\boldsymbol{x}, \eta(\boldsymbol{x}, t), t)$, through $b(\boldsymbol{k}, t)$ where

$$\hat{\eta}(\boldsymbol{k}, t) = (\omega/2g)^{\frac{1}{2}}[b(\boldsymbol{k}, t) + b^*(-\boldsymbol{k}, t)], \tag{2.4a}$$

$$\hat{\phi}^s(\boldsymbol{k}, t) = -\mathrm{i}(g/2\omega)^{\frac{1}{2}}[b(\boldsymbol{k}, t) - b^*(-\boldsymbol{k}, t)], \tag{2.4b}$$

and

$$b(\boldsymbol{k}, t) = [B + B' + B'' + B''' + \ldots]\, \mathrm{e}^{-\mathrm{i}\omega(\boldsymbol{k})t}. \tag{2.4c}$$

The quantities $B', B'', \ldots$, are the *bound components* of the wave field, which are given in terms of B by equations such as

$$\begin{aligned} B' = -\int\int_{-\infty}^{\infty} \Bigg\{ & V^{(1)}_{0,1,2}\, B_1 B_2\, \delta(\boldsymbol{k}-\boldsymbol{k}_1-\boldsymbol{k}_2)\frac{\mathrm{e}^{\mathrm{i}(\omega-\omega_1-\omega_2)t}}{\omega-\omega_1-\omega_2} + V^{(2)}_{0,1,2}\, B_1^* B_2\, \delta(\boldsymbol{k}+\boldsymbol{k}_1-\boldsymbol{k}_2) \\ & \times \frac{\mathrm{e}^{\mathrm{i}(\omega+\omega_1-\omega_2)t}}{\omega+\omega_1-\omega_2} + V^{(3)}_{0,1,2}\, B_1^* B_2^*\, \delta(\boldsymbol{k}+\boldsymbol{k}_1+\boldsymbol{k}_2)\frac{\mathrm{e}^{\mathrm{i}(\omega+\omega_1+\omega_2)t}}{\omega+\omega_1+\omega_2} \Bigg\}\, \mathrm{d}\boldsymbol{k}_1\, \mathrm{d}\boldsymbol{k}_2. \end{aligned} \tag{2.5}$$

We consider two-dimensional standing waves (independent of y) in the present investigation, in a deep tank with walls at $x = 0, l$. The end conditions are

$$\phi_x(0) = \phi_x(l) = 0, \tag{2.6}$$

and $B(\boldsymbol{k}, t)$ has the discrete structure

$$B(\boldsymbol{k}, t) = \sum_{m=1}^{M} B_m(t)\,[\delta(\boldsymbol{k} - mk\boldsymbol{i}) + \delta(\boldsymbol{k} + mk\boldsymbol{i})], \tag{2.7}$$

where $k = \pi/l$ and $\boldsymbol{i}$ is the unit vector in the x-direction. The upper bound M is set to ensure that the sum stays within the gravity wave regime.

2.2. *Linear and weakly nonlinear theory*

The general solution of the linearized two dimensional version of (2.1) or (2.2) with the end conditions (2.6) is

$$\eta = \sum_{m=1}^{M} a_m \cos(mkx) \cos[(mgk)^{\frac{1}{2}} t + \tau_m], \tag{2.8a}$$

$$\phi = \sum_{m=1}^{M} -\left(\frac{g}{mk}\right)^{\frac{1}{2}} a_m \, \mathrm{e}^{mkz} \cos(mkx) \sin[(mgk)^{\frac{1}{2}} t + \tau_m]. \tag{2.8b}$$

Each of the terms in (2.8*a*) is a *free component*, with amplitude a_m and phase τ_m. The steepness mka_m of each free component is of order $\epsilon \ll 1$ to justify the use of weakly nonlinear theory.

The general series (2.8*a*, *b*) consist of standing waves with a common wavelength $2l$ and a range of periods. We focus here on standing waves for which the motion is strictly periodic in time with a period T where $T = 2(\pi l/g)^{\frac{1}{2}}$, which we call *pure standing waves*. They are obtained when $a_m = 0$ for all m except when $m = n^2, n = 1, 2, \ldots,$ and are given by

$$\eta = \sum_{n=1}^{N} a_{n^2} \cos(n^2 kx) \cos[n(gk)^{\frac{1}{2}} t + \tau_{n^2}], \tag{2.9a}$$

$$\phi = \sum_{n=1}^{N} -\frac{1}{n}\left(\frac{g}{k}\right)^{\frac{1}{2}} a_{n^2} \, \mathrm{e}^{n^2 kz} \cos(n^2 kx) \sin[n(gk)^{\frac{1}{2}} t + \tau_{n^2}]. \tag{2.9b}$$

A large variety of standing waves of this type is possible because of the large range of possible values for a_{n^2} and τ_{n^2}.

Weakly nonlinear interactions produce standing wave solutions containing the series (2.8*a*, *b*) (or (2.9*a*, *b*)) except that a_m and τ_m are functions of the slow times $t_p = \epsilon^p t$, $p = 2, 3, \ldots$. The weakly nonlinear solutions also include the *bound components* composed from double, triple, ... products of the free components. For weakly nonlinear pure standing waves to exist with a strict periodicity like their linear counterpart (2.9*a*, *b*), it is necessary that a_{n^2} is independent of time and that τ_{n^2} has a specific time dependence. This constraint imposes selection criteria for a_{n^2} from the third-order theory and for τ_{n^2} from the fifth-order theory, which are derived in §§2.3 and 2.4 respectively.

The above weakly nonlinear standing waves also have slowly varying forms in which a_{n^2} and τ_{ν^2} are functions of the slow times, $t_p = \epsilon^p t, p = 2, 3, \ldots$. Sideband instability which brings in the components a_m for $m = n^2 \pm 1, n = 2, 3, \ldots$ produces slowly varying standing waves of this type. This phenomenon is discussed in §2.5.

2.3. *Third-order (Zakharov's) theory*

We consider weakly nonlinear pure standing waves containing three free components for which

$$B(\boldsymbol{k}, t) = \sum_{n=1}^{3} B_{n^2}[\delta(\boldsymbol{k} - n^2 k\boldsymbol{i}) + \delta(\boldsymbol{k} + n^2 k\boldsymbol{i})], \tag{2.10a}$$

where
$$B_{n^2} = A_{n^2}\,\mathrm{e}^{-\mathrm{i}n\Omega t+\mathrm{i}\phi_{n^2}} \tag{2.10b}$$

and A_{n^2}, Ω, ϕ_{n^2} are all real constants with $A_{n^2} > 0$. The period of this standing wave is

$$T = \frac{2\pi}{(gk)^{\frac{1}{2}}+\Omega}. \tag{2.11}$$

We set $\phi_1 = 0$, without loss of generality.

Substitution of (2.10) into (2.2) with $I_p = 0, p > 3$ (Zakharov's equation) yields

$$\Omega A_1 = [(T_{1111}+2T_{1\bar{1}1\bar{1}})A_1^2+2(T_{1414}+T_{14\bar{1}\bar{4}})A_4^2+2(T_{1919}+T_{19\bar{1}\bar{9}})A_9^2]A_1 + T_{19\bar{4}\bar{4}}A_4^2 A_9\,\mathrm{e}^{\mathrm{i}(2\phi_4-\phi_9)}, \tag{2.12a}$$

$$2\Omega A_4 = [2(T_{4141}+T_{4\bar{1}4\bar{1}})A_1^2+(T_{4444}+2T_{44\bar{4}\bar{4}})A_4^2+2(T_{4949}+T_{49\bar{4}\bar{9}})A_9^2]A_4 + 2T_{449\bar{1}}A_1 A_4 A_9\,\mathrm{e}^{-\mathrm{i}(2\phi_4-\phi_9)}, \tag{2.12b}$$

$$3\Omega A_9 = [2(T_{9191}+T_{9\bar{1}9\bar{1}})A_1^2+2(T_{9494}+T_{94\bar{9}\bar{4}})A_4^2+2(T_{9999}+T_{99\bar{9}\bar{9}})A_9^2]A_9 + 2T_{9\bar{1}44}A_1 A_4^2\,\mathrm{e}^{\mathrm{i}(2\phi_4-\phi_9)}. \tag{2.12c}$$

The subscript notation is best explained by the example

$$T_{9\bar{1}44} = T(9k\boldsymbol{i}, -k\boldsymbol{i}, 4k\boldsymbol{i}, 4k\boldsymbol{i}).$$

Most of the coefficients in the above system (2.12) are either zero or cancel each other owing to the symmetry of the problem, leaving the substantial simplification

$$\Omega A_1 = -\frac{k^3}{4\pi^2}A_1^3, \qquad 2\Omega A_4 = -\frac{64k^3}{4\pi^2}A_4^3, \qquad 3\Omega A_9 = -\frac{729k^3}{4\pi^2}A_9^3. \tag{2.13a–c}$$

The standing Stokes wave is a solution of (2.13) if $A_4 = A_9 = 0$, when the well-known result is obtained:

$$\Omega = -\frac{k^3}{4\pi^2}A_1^2 = -(gk)^{\frac{1}{2}}\frac{(ka_1)^2}{8}. \tag{2.14a}$$

This derivation uses the relation

$$a_m^2 = 2\left(\frac{mk}{g}\right)^{\frac{1}{2}}\frac{A_m^2}{\pi^2} \tag{2.14b}$$

from Stiassnie & Shemer (1984).

The system (2.13) admits four additional non-trivial solutions.

(i) For $A_9 = 0$, elimination of Ω between (2.13*a*) and (2.13*b*) gives

$$(A_4/A_1)^2 = \tfrac{1}{32}, \quad a_4/a_1 = \tfrac{1}{4}, \tag{2.15}$$

with Ω the same as in (2.14).

(ii) For $A_4 = 0$, elimination of Ω between (2.13*a*) and (2.13*c*) gives

$$(A_9/A_1)^2 = \tfrac{1}{243}, \quad a_9/a_1 = \tfrac{1}{9}, \tag{2.16}$$

with Ω the same as in (2.14).

(iii) Equations (2.14), (2.15), and (2.16) remain valid for the more general case in which all three waves coexist. This result is easily generalized for $N > 3$.

(iv) Another solution is possible for $A_1 = 0$. Elimination between (2.13*b*) and (2.13*c*) for this case yields

$$\Omega = -\frac{8k^3}{\pi^2} A_4^2 = -2(gk)^{\frac{1}{2}}(ka_4)^2, \tag{2.17a}$$

$$(A_9/A_4)^2 = \tfrac{32}{243}, \quad a_9/a_4 = \tfrac{4}{9}. \tag{2.17b}$$

Zakharov's equation, containing the lowest significant order of nonlinearity, enables specific values to be obtained for the wave amplitudes a_{n^2}. It does not provide any information about the phases ϕ_{n^2}. For this, it is necessary to go to higher nonlinearities using the modified Zakharov equation and its extensions.

2.4. *Higher-order nonlinearity*

Substitution of (2.10) into (2.2) with $I_p = 0, p > 4$ (modified Zakharov's equation) yields

$$\Omega A_1 = -\frac{k^3}{4\pi^2} A_1^3 + [U^{(2)}_{14\bar{1}\bar{1}1}\, \mathrm{e}^{-\mathrm{i}\phi_4} + (U^{(3)}_{11114} + U^{(3)}_{1114\bar{1}})\, \mathrm{e}^{\mathrm{i}\phi_4}] A_1^3 A_4, \tag{2.18a}$$

$$2\Omega A_4 = -\frac{64k^3}{4\pi^2} A_4^3 + U^{(2)}_{41111}\, \mathrm{e}^{-\mathrm{i}\phi_4} A_1^4, \tag{2.18b}$$

$$3\Omega A_9 = -\frac{729k^3}{4\pi^2} A_9^3. \tag{2.18c}$$

Note that at this order of nonlinearity and for the three chosen components A_1, A_4, A_9, there is no additional coupling between the component A_9 and the other two. The new coupling between A_1 and A_4 could in principle produce information about the phase ϕ_4 and produce a correction to (2.15). However, symbolic computation (with Maple) of $U^{(2)}_{14\bar{1}\bar{1}\bar{1}}$, $U^{(2)}_{41111}$ and the sum $U^{(3)}_{1111\bar{4}} + U^{(3)}_{1114\bar{1}}$ show that all are exactly zero, so that there is no contribution of the new terms to the right-hand side of (2.18).

The sextet nonlinear interaction term, I_5, in (2.2) has a similar structure to that of I_3 and I_4 in (2.3*a*, *b*), with unknown real kernels which we denote by $Q_{0,1,2,3,4,5}$. This order modifies the structure of the system (2.18). An important part of the modification arises from the term

$$Q_{44\bar{1}1\bar{1}\bar{1}}\, \mathrm{e}^{-2\mathrm{i}\phi_4} A_1^4 A_4 \tag{2.19}$$

on the right-hand side of (2.18*b*). (The exponent $-2\mathrm{i}\phi_4$ in (2.19) is a combination of the exponent $-\mathrm{i}\phi_4$ in the term $B_4^* B_1^2 B_1^2$ of I_5 on the right-hand side of (2.2) and the exponent $\mathrm{i}\phi_4$ from B_4 on the left-hand side of (2.2).) A necessary condition for a pure standing wave is therefore

$$2\phi_4 = m\pi, \quad m = 0, \pm 1, \pm 2, \ldots, \tag{2.20}$$

which yields four different solutions having $\phi_4 = 0, \frac{1}{2}\pi, \pi, \frac{3}{2}\pi$, which we denote by standing waves SA, SB, SC, SD respectively. (The letter S indicates that the amplitude a_1 has a value comparable with that for the Stokes standing waves, and the second letter follows the notation of Agnon *et al.* 1992 for the value of ϕ_4.) Note that the result (2.20) relies on the assumption that $Q_{44\bar{1}1\bar{1}\bar{1}} \neq 0$, an assumption which is consistent with the numerical calculation of the four different solutions (§4.2). The space–time perspective of the standing wave SA over half of a wave period is compared with the corresponding perspective of the Stokes standing wave S in figure 1.

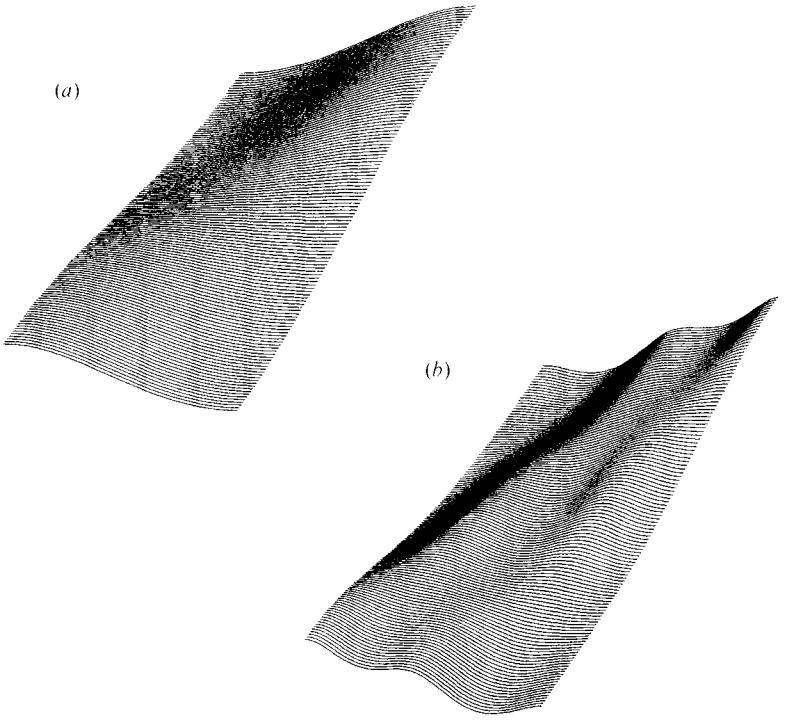

FIGURE 1. The space–time perspectives of (*a*) the S and (*b*) the SA standing waves with $\epsilon = 0.1$, vertical magnification π. The length l between the vertical walls (half the fundamental wavelength) is drawn across the page, and half the fundamental period is shown up the page.

These different types of standing waves were first described by Agnon *et al.* (1992). For $A_4 = 0$, $A_1, A_9 \neq 0$ only the two types of standing waves for which $\phi_9 = 0, \pi$ are found to occur, and are denoted by standing waves SNA, SNC respectively. (The letter N indicates that the amplitude a_4 is almost null.) We use numerical solutions of the full nonlinear wave problem in order to calculate these and other new forms of nonlinear standing waves and to investigate their stability.

2.5. *Linear stability*

The linear stability of the new waves to small disturbances at adjoining wavenumbers is studied next. Two cases are considered.

(i) Class I instability of the wave having components A_1 and A_9 with disturbances at $k_8 = 8k$ and $k_{10} = 10k$. This instability has the timescale $t_2 = \epsilon^2 t$. The governing equations are

$$\mathrm{i}\frac{\mathrm{d}B_8}{\mathrm{d}t} = T_{8\,10\,9\,9}\, B_{10}^* B_9^2\, \mathrm{e}^{-\mathrm{i}(2\omega_9 - \omega_8 - \omega_{10})t}, \tag{2.21a}$$

$$\mathrm{i}\frac{\mathrm{d}B_{10}}{\mathrm{d}t} = T_{10\,8\,9\,9}\, B_8^* B_9^2\, \mathrm{e}^{-\mathrm{i}(2\omega_9 - \omega_8 - \omega_{10})t}, \tag{2.21b}$$

where B_9 is given by (2.10*b*) with (2.14*a*, *b*) and (2.16). Following Stiassnie & Shemer (1984) or Okamura (1984), the range of steepness for instability, which is found to be independent of ϕ_9 and thus the same for the standing waves SNA and SNC, is given by

$$0.0812 < ka_1 < 0.3239. \tag{2.21c}$$

(ii) Class I combined with Class II instability of the wave having components A_1 and A_4 with disturbances at $k_3 = 3k$ and $k_5 = 5k$. This instability depends on two timescales, $t_2 = \epsilon^2 t$ and $t_3 = \epsilon^3 t$. The governing equations are

$$\mathrm{i}\frac{\mathrm{d}B_3}{\mathrm{d}t} = T_{3544} B_5^* B_4^2 \, \mathrm{e}^{-\mathrm{i}(2\omega_4-\omega_3-\omega_5)t} + (U^{(2)}_{35\bar{4}\bar{1}1} + U^{(2)}_{351\bar{4}1} + U^{(2)}_{3511\bar{4}}) B_5^* B_4 B_1^2 \, \mathrm{e}^{-\mathrm{i}(2\omega_1+\omega_4-\omega_3-\omega_5)t}, \tag{2.22a}$$

$$\mathrm{i}\frac{\mathrm{d}B_5}{\mathrm{d}t} = T_{5344} B_3^* B_4^2 \, \mathrm{e}^{-\mathrm{i}(2\omega_4-\omega_3-\omega_5)t} + (U^{(2)}_{53\bar{4}\bar{1}1} + U^{(2)}_{531\bar{4}1} + U^{(2)}_{5311\bar{4}}) B_3^* B_4 B_1^2 \, \mathrm{e}^{-\mathrm{i}(2\omega_1+\omega_4-\omega_3-\omega_5)t}, \tag{2.22b}$$

where B_1 and B_4 are given by (2.10b) and (2.14a, b), (2.15). The range of steepness for instability depends on ϕ_4. The standing wave SA is found to be unstable for

$$0.2031 < ka_1 < 0.3354, \tag{2.22c}$$

the standing wave SC for

$$0.1844 < ka_1, \tag{2.22d}$$

and the standing waves SB and SD are always unstable.

Both systems (2.21) and (2.22) represent cases of near-resonant interaction.

3. Computation

3.1. *Governing equations*

The dimensional quantities of the previous section are all made non-dimensional for the purpose of computation. Lengths are made non-dimensional with respect to l/π, where l is the distance between the vertical walls, so that the standing wave motion takes place between the vertical planes $x = 0$ and $x = \pi$. Times are made non-dimensional with respect to the inverse of the lowest linear frequency $(\pi g/l)^{\frac{1}{2}}$. The displacement of the water surface is written $z = \eta(x, t)$ and the water motion is assumed to be irrotational with the non-dimensional velocity potential $\phi(x, z, t)$. This satisfies Laplace's equation

$$\phi_{xx} + \phi_{zz} = 0, \quad z \leqslant \eta, \tag{3.1a}$$

with $\phi_x = 0$ on $x = 0$ and $x = \pi$, and $\phi_z \to 0$ as $z \to -\infty$. The nonlinear boundary conditions on the water surface are the kinematic condition

$$\eta_t - \phi_z + \eta_x \phi_x = 0 \quad \text{on} \quad z = \eta, \tag{3.1b}$$

and the dynamic condition

$$\phi_t + \eta + \tfrac{1}{2}(\phi_x^2 + \phi_z^2) = 0 \quad \text{on} \quad z = \eta. \tag{3.1c}$$

One of the simplest nonlinear solutions is that for two-dimensional *pure standing waves*. Their Fourier series expansions (before truncation) are

$$\eta = \sum_{m=1}^{\infty} \sum_{n=m \bmod 2}^{\infty} \cos mx (a_{mn} \cos n\omega t + b_{mn} \sin n\omega t), \quad m+n \text{ even}, \tag{3.2a}$$

and

$$\phi = \sum_{m=1}^{\infty} \sum_{n=m \bmod 2}^{\infty} \cos mx \, \mathrm{e}^{mz} (c_{mn} \cos n\omega t + d_{mn} \sin n\omega t), \quad m+n \text{ even}, \tag{3.2b}$$

where the coefficients $a_{mn}, b_{mn}, c_{mn}, d_{mn}$ are constants, and $\omega (\sim 1)$ is the nonlinear

frequency of the fundamental harmonic. The constraint that $m+n$ is even is a consequence of the invariance of η and ϕ when x and ωt are both changed by π.

A number of measures of the non-dimensional standing wave amplitude have been used previously. Solutions of Zakharov's equation have often used the steepness of the fundamental harmonic, a_{11}, while Schwartz & Whitney (1981) use half of the non-dimensional wave height at $t = 0$, which in the present notation is

$$\epsilon_{SW} = \sum_{m=1}^{\infty} \sum_{n=1}^{\infty} a_{mn}, \quad m, n, \text{odd}. \tag{3.3}$$

In order to reflect the fact that the present standing waves can have harmonics with local amplitude maxima at other than the fundamental harmonic, with phases different from that of the fundamental harmonic, the non-dimensional root-mean energy is chosen as the measure of wave amplitude. It is

$$\epsilon = \left(\frac{2}{\pi}\int_0^{\pi}\left(\phi(x,\eta,t)\frac{\partial\eta}{\partial t}+\eta^2\right)\mathrm{d}x\right)^{\frac{1}{2}} \tag{3.4}$$

(West 1981, pp. 32–34), which is independent of t because of the conservation of energy. Note that $\epsilon \sim a_{11}$ in the linear limit of a standing wave at the fundamental harmonic (with phase zero) only.

3.2. *Pure standing wave solutions (fixed-point method)*

When the Fourier series (3.2*a*, *b*) are substituted into (3.1*b*, *c*), denoted by $F = 0, G = 0$ respectively, the resulting equations may be rewritten

$$F = \sum_{M=1}^{\infty} \sum_{N=M \bmod 2}^{\infty} \cos Mx(A_{MN}\cos N\omega t + B_{MN}\sin N\omega t) = 0, \quad M+N \text{ even}, \tag{3.5a}$$

and

$$G = \sum_{M=1}^{\infty} \sum_{N=M \bmod 2}^{\infty} \cos Mx(C_{MN}\cos N\omega t + D_{MN}\sin N\omega t) = 0, \quad M+N \text{ even}, \tag{3.5b}$$

where the coefficients $A_{MN}, B_{MN}, C_{MN}, D_{MN}$ are functions of the coefficients $a_{mn}, b_{mn}, c_{mn}, d_{mn}$ and the frequency ω. The function dependence could be found, but this is unnecessary for the calculation of numerical solutions. The Fourier series (3.2*a*, *b*) are also substituted into the normalizing equation (3.4) rewritten to the left-hand side, which is then denoted by $H = 0$, and is a function of $a_{mn}, b_{mn}, c_{mn}, d_{mn}$ and ω also. This description assumes the usual calculation in which the root-mean energy ϵ is given and the quantities $a_{mn}, b_{mn}, c_{mn}, d_{mn}$ and ω have to be found for a particular family of standing wave solutions. It takes only a simple re-ordering of the method if, instead, one of the latter quantities is given and ϵ is included among the quantities that have to be found.

Particular numerical values for the coefficients $a_{mn}, b_{mn}, c_{mn}, d_{mn}$ and ω are inserted into truncated versions of the Fourier series (3.2*a*, *b*), the series are substituted into (3.1*b*, *c*), (3.4) over an array of points in x and t, and numerical values of the coefficients $A_{MN}, B_{MN}, C_{MN}, D_{MN}$ are calculated from truncated versions of (3.5*a*, *b*) by the fast Fourier transform method. The partial derivatives of $A_{MN}, B_{MN}, C_{MN}, D_{MN}$ with respect to $a_{mn}, b_{mn}, c_{mn}, d_{mn}$ and ω are calculated numerically by the same method, and the Jacobian is formed from these derivatives and from the partial derivatives of H. The numerical values of $a_{mn}, b_{mn}, c_{mn}, d_{mn}$ and ω are improved then by Newton's method until $A_{MN}, B_{MN}, C_{MN}, D_{MN}, H$ are as close to zero as is required

(typically 10^{-5} was found to be adequate). At the same time, the number of terms included in the truncated series may be increased until the residuals in (3.5*a*, *b*) from terms not included are also as close to zero as is required.

The calculations are started when ϵ is sufficiently small that the coefficients $a_{mn}, b_{mn}, c_{mn}, d_{mn}$ may be given by linear values with $\omega = 1$ as an initial approximation. Each solution for the coefficients is then used as an initial approximation to the next solution as ϵ is increased. A typical solution for the new standing waves at $\epsilon \sim 0.1$ with the above numerical precision has about 90 harmonics ($m \leqslant 20, n \leqslant 9$), needing 360 amplitudes. The method of solution described above has evolved from one developed originally for three-dimensional permanent waves on deep water (Bryant 1985). The generalization of the method to calculations of the nonlinear time evolution is described next.

3.3. *Non-periodic standing waves (time evolution method)*

The displacement, $\eta(x, t)$, and velocity potential, $\phi(x, z, t)$, are expanded now in Fourier series in x, with Fourier coefficients dependent on t, to yield (before truncation)

$$\eta = \sum_{m=1}^{\infty} a_m(t) \cos mx, \tag{3.6a}$$

and

$$\phi = \sum_{m=1}^{\infty} b_m(t)\, \mathrm{e}^{mz} \cos mx. \tag{3.6b}$$

When the Fourier series (3.6*a*, *b*) are substituted into (3.1*b*, *c*), these equations may be rewritten, following (3.5*a*, *b*), in the form

$$F = \sum_{M=1}^{\infty} A_M(t) \cos Mx = 0 \quad \text{and} \quad G = \sum_{M=1}^{\infty} B_M(t) \cos Mx = 0, \tag{3.7a, b}$$

where the coefficients $A_M(t), B_M(t)$ are functionals of $a_m(t), b_m(t)$. Each of the coefficients $A_M(t), B_M(t)$, when equated to zero, is an implicitly-defined first-order nonlinear ordinary differential equation for the corresponding Fourier coefficient of (3.6*a*, *b*) in terms of all Fourier coefficients of (3.6*a*, *b*). It is extracted numerically from (3.7*a*, *b*) by the fast Fourier transform method. The set of differential equations obtained by equating all coefficients $A_M(t), B_M(t)$ to zero is solved numerically using an integrater devised for initial value problems in stiff systems of implicit ordinary differential equations (NAG subroutine D02NGF), with a local error tolerance of 10^{-11}. The differential equations are implicit because the exponential multipliers in (3.6*b*) are evaluated on the surface given by (3.6*a*).

The root-mean energy (3.4) is calculated regularly as a check on the computation. In a number of the examples, the nonlinear interactions between the harmonics cause a slow transfer of energy to the higher harmonics. This results in a buildup of energy in the truncation harmonics, causing the total energy to increase and the calculations to fail. It is only a partial remedy to include more harmonics because it may only postpone the failure, and it may introduce rounding errors from the exponential multipliers in (3.6*b*) at large wavenumbers.

The Fourier amplitudes calculated in (3.6*a*, *b*) evolve in fast time. These Fourier expansions are interpreted more easily if the fast time variation is removed by Fourier decomposition over each fundamental period $2\pi/\omega$, to yield (before truncation)

$$\eta = \sum_{m=1}^{\infty} \sum_{n=0}^{\infty} a_{mn}(t) \cos mx \cos(n\omega t + \alpha_{mn}(t)), \tag{3.8a}$$

and $$\phi = \sum_{m=1}^{\infty} \sum_{n=0}^{\infty} c_{mn}(t) \cos mx \, e^{mz} \cos(n\omega t + \gamma_{mn}(t)), \tag{3.8b}$$

where the amplitudes and phases are now functions of slow time. (It should be noted that the amplitudes a_{mn}, c_{mn} defined in (3.8*a*, *b*) differ from those defined in (3.2*a*, *b*) unless the phases are all zero.)

The nonlinear time evolution calculations are used to investigate the stability of pure standing wave solutions because they do not make the constant amplitude and phase assumptions implicit in linear stability analyses. The time evolution calculations are based on a numerical method independent of that used for the fixed-point calculations, so that consistency between the properties obtained from the two sets of calculations increases confidence in both.

4. Standing wave examples

4.1. *Standing waves with Stokes ordering*

The pure standing waves calculated originally by Rayleigh (1915), and improved to high order by Schwarz & Whitney (1981), have an ordering of harmonic amplitudes similar to that of the Stokes progressive waves, and are named Stokes standing waves below (denoted by S). The amplitudes decrease monotonically, in general, as their wavenumber m and frequency $n\omega$ increase.

The fixed-point computational method (§3.2) converges rapidly to the Stokes standing wave solutions with high numerical precision (error $< 10^{-10}$), up to $\epsilon = 0.2$. Solutions at larger values of ϵ are not included here because of the convergence difficulties associated with the exponential multipliers in (3.2*b*) at high wavenumbers. By choosing the time origin so that the phase of the fundamental harmonic α_{11} is zero, all the Fourier sine coefficients in (3.2*a*, *b*) are also zero. The frequency ω, expanded as a polynomial in the fundamental amplitude a_{11} over the range $0 < \epsilon < 0.2$ (using the NAG subroutine E02ADF), is found to have the leading terms

$$\omega = 1.000000 - 0.1250 a_{11}^2 + \ldots. \tag{4.1a}$$

These are consistent with (2.11) and (2.14*a*), and the corresponding expansion for $1/\omega^2$ in terms of ϵ_{SW} (defined in (3.3)) agrees with the leading terms of Schwarz & Whitney, equation (3.2). For the purpose of comparison with later expansions, the leading term of the expansion for the amplitude a_{42} is given by

$$a_{42} = 0.19 a_{11}^4 + \ldots. \tag{4.1b}$$

Although the Stokes standing waves are generally regarded as being stable to superharmonic disturbances at small to moderate amplitudes, they are unstable to subharmonic disturbances such as those described in (2.21*a*–*c*). The instability range (2.21*c*) suggests that if a set of nine Stokes standing waves is generated between the vertical walls, with $\epsilon = 0.1$ for each wave, the set is unstable to sideband disturbance at wavenumbers 8 and 10. Initial conditions were chosen to consist of these nine standing waves perturbed by a disturbance of amplitude 10^{-5} at wavenumber 1, and their time evolution was calculated to confirm the initial linear instability and to find the form of the evolving standing wave motion. (An initial disturbance is introduced here, rather than leaving it to arise from numerical error as is done in all the following examples, because all the disturbance harmonics have exactly zero initial amplitudes otherwise. The initial disturbance chosen is approximately equal to the rounding error in the other examples.)

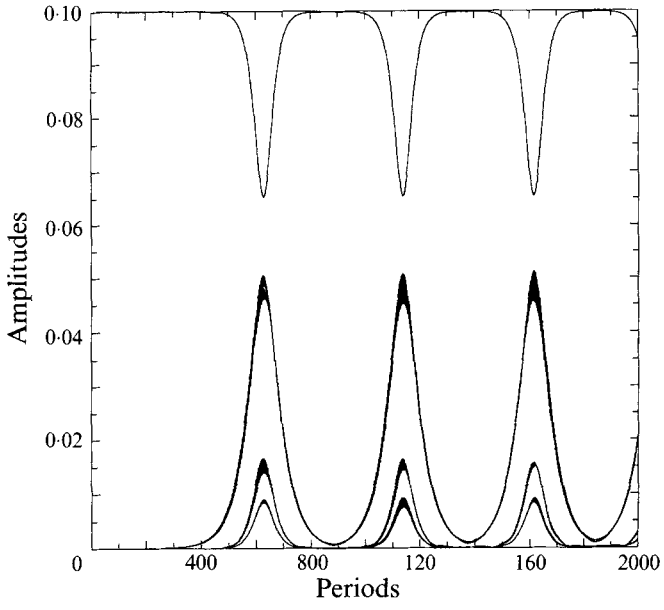

FIGURE 2. The sideband modulation of a set of nine Stokes standing waves, where $\epsilon = 0.1$ for each. The cyclic recurrence in slow time results from the instability of the Stokes standing waves to a subharmonic disturbance. The fundamental amplitude a_{93} of each of the original standing waves is at the top, then in order the two sideband amplitudes a_{83} and a_{103} are almost superposed, followed in order by the sideband amplitudes a_{113} and a_{73}.

The expansions (3.6a, b) are modified to

$$\eta = \sum_{m=1}^{45} a_m(t)\cos\tfrac{1}{9}mx, \quad \phi = \sum_{m=1}^{45} b_m(t)\,\mathrm{e}^{mz/9}\cos\tfrac{1}{9}mx, \tag{4.2a, b}$$

because the standing wave motion takes place between $x = 0$ and $x = 9\pi$. The fast-time variation of the coefficients is removed by Fourier expansion over the corresponding period $6\pi/\omega$, as in (3.8a, b), to yield

$$\eta = \sum_{m=1}^{45}\sum_{n=0}^{9} a_{mn}(t)\cos\tfrac{1}{9}mx\cos(\tfrac{1}{3}n\omega t + \alpha_{mn}(t)), \tag{4.2c}$$

and

$$\phi = \sum_{m=1}^{45}\sum_{n=0}^{9} c_{mn}(t)\cos\tfrac{1}{9}mx\,\mathrm{e}^{mz/9}\cos(\tfrac{1}{3}n\omega t + \gamma_{mn}(t)), \tag{4.2d}$$

where the amplitudes and phases are now functions of slow time. (The chosen upper limits for the series are a balance between the needs for sufficient numerical precision and sufficient computational speed.)

The slow-time evolution of the Stokes standing waves is illustrated in figure 2, which shows the fundamental amplitude a_{93} of each of the original standing waves at the top, then in order the two sideband amplitudes a_{83} and a_{103} almost superposed, followed in order by the sideband amplitudes a_{113} and a_{73}. The standing wave system is exhibiting cyclic recurrence, of similar form to that found for Stokes progressive waves (Lake *et al.* 1977). The system retains its initial Fourier amplitudes for about 400 wave periods while the linear instability gathers strength, then the amplitudes undergo the slow nonlinear modulation described usually as cyclic recurrence. The period and the amplitude of the nonlinear modulation cycles are nearly constant. Each modulation

cycle consists of about 250 wave periods in which the amplitudes remain close to their initial values and about 250 wave periods in which the wave amplitudes change more rapidly. The root-mean energy (3.4) decreases by about 1 % over the 2000 wave periods in the figure owing to the energy losses at the truncation of the series (4.2).

In order to understand the nonlinear interactions better, the Fourier coefficients $a_m(t)$ in (4.2*a*), calculated in fast time over the complete modulation cycle of length 514 wave periods from period 626 to period 1140, are decomposed into Fourier series of period equal to the 514 wave periods. (This Fourier decomposition, being over the large number 514×64 of points, is almost equivalent to regarding the frequencies as forming a continuum.) Most of the energy at wavenumber $n = 9$ is found to be in a dominant waveband centred on frequency $n = 3$, as is expected from the initial conditions. However, the energy at the sideband wavenumber $m = 8$ is found to be mostly in a dominant waveband centred near the linear frequency $\omega(8) = \sqrt{8}$, rather than near the frequencies $n = 2$ and $n = 4$ expected from (3.2*a*, *b*). The reason for the occurrence of the linear frequency is that the dominant sideband wave component is a *free component*, as defined in (2.2), not a *bound component* such as those in (3.2*a*, *b*). Bound components are found at this wavenumber, such as that at the frequency $2\omega(9) - \omega(8) = 6 - \sqrt{8}$, but they have much less energy than the free component. Most of the energy at the other sideband wavenumbers $m = 7, 10, 11$ is also found in the free components with wavebands centred near $\omega(m) = m^{\frac{1}{2}}, m = 7, 10, 11$ respectively.

4.2. *Standing waves with resonating first and fourth harmonics*

The weakly nonlinear theory predicts that pure standing waves exist for which the first and fourth harmonics interact resonantly with the amplitude ratio (2.15)

$$a_{42}/a_{11} = \tfrac{1}{4}$$

in the present notation (3.8*a*, *b*). The phase α_{42} relative to the phase α_{11} (2.20) may be $0, \frac{1}{2}\pi, \pi, \frac{3}{2}\pi$, denoted by standing waves SA, SB, SC, SD respectively. The letter S indicates that, like the Stokes standing wave, the amplitude a_{11} is dominant, and the second letter denotes the phase α_{42} relative to α_{11}. Standing waves of types SA and SC are described first.

The fixed-point computational method (§3.2) converges rapidly to these standing wave solutions with high numerical precision (error $< 10^{-10}$), up to $\epsilon = 0.2$. Like the Stokes standing waves, the time origin may be chosen so that all the Fourier sine coefficients in (3.2*a*, *b*) are zero. In order to check the predictions of the weakly nonlinear theory, the frequency ω and resonant amplitude a_{42} are expanded as polynomials in the fundamental amplitude a_{11} over the range $0 < \epsilon < 0.05$. They are found to have the leading terms

$$\omega = 1.000000 - 0.1250a_{11}^2 + \ldots \quad \text{and} \quad a_{42} = 0.25000a_{11} - 0.875a_{11}^3 + \ldots, \quad (4.3a, b)$$

for both the SA and SC waves. The phase α_{42} (relative to α_{11}) is zero for the SA waves and π for the SC waves. The expansions confirm (2.14*a*) and (2.15), and (4.3*b*) has important differences from the corresponding expansion (4.1*b*) for Stokes standing waves. Equation (4.1*b*) begins with the fourth power, consistent with the Stokes ordering, while (4.3*b*) has linear and cubic leading terms due to the resonant interaction between the first and fourth harmonics. Apart from the maximum at a_{42}, the remaining harmonic amplitudes for the SA and SC waves lie close to a Stokes ordering.

The stability of the standing waves for root-mean energies in the range $0 < \epsilon < 0.2$ is determined by calculating their long-time evolution (§3.3) for up to 10000 wave

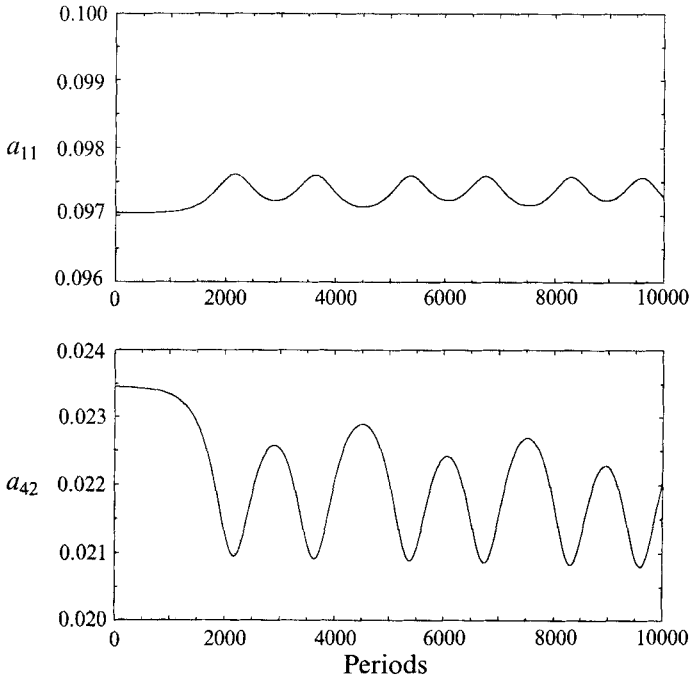

FIGURE 3. The time evolution of the resonant amplitudes a_{11} and a_{42}, starting from the standing wave SA with $\epsilon = 0.1$.

periods. At $\epsilon = 0.05$, the harmonic amplitudes of both the SA and SC waves stay almost constant over the 10000 wave periods, but the phase α_{42} of the dominant fourth component relative to the phase α_{11} of the dominant first component drifts monotonically by more than π over the same long time. This property is probably associated with the fact that the amplitudes are determined at the third order (2.15), but the phases are determined at the fifth order (2.19).

An unexpected long-time behaviour occurs when the root-mean energy is increased to $\epsilon = 0.1$. The linear stability analysis for this case (2.27*a–c*) indicates that the standing waves SA and SC at this energy are stable. The stability described by this analysis may be demonstrated by starting from the fixed-point standing wave SA solution with a standing wave disturbance 0.01 added to the resonant amplitude a_{42} and -0.005 to the associated velocity potential amplitude, when all amplitudes oscillate in an apparent linearly stable motion with a period about 200 wave periods. However, the time evolution of the wave SA illustrated in figure 3, starting from the fixed-point standing wave solution with the only disturbance being the initial numerical error, shows that the wave SA is unstable. It shows also that the amplitudes of its dominant harmonics evolve into slow modulated nonlinear oscillations.

When the fast-time variation of the sideband amplitudes in (3.6*a*, *b*) is decomposed with respect to one modulation period equal to 3160 wave periods (effectively a Fourier decomposition into a continuum of frequencies), it is found that the energy in the sideband wave components occurs dominantly in wavebands centred near the *bound components* with amplitudes $a_{31}, a_{33}, a_{51}, a_{53}$, consistent with (3.2*a*, *b*). Unlike the sideband modulation in §4.1 or in the system (2.22), the energy in the *free components* of the sidebands does not rise above the background level here. This means that the sideband wave components play only a passive role in the nonlinear modulation

illustrated in figure 3, with the primary nonlinear interaction being that between the dominant resonating free components with amplitudes a_{11} and a_{42}. We do not have a theoretical model yet to describe the instability leading to this nonlinear modulation.

Another property shown by figure 3 is that the standing wave SA is only marginally unstable. The time evolution illustrated in this figure is started from the fixed-point standing wave solution, with the only disturbance being the initial numerical error. It can be seen that the standing wave amplitudes remain near their initial values for about 1000 wave periods before evolving into the nonlinear modulated oscillations. Although not shown in the figure, the phases also remain constant over the same 1000 wave periods. The root-mean energy ϵ decreases by only 0.1 % over the 10000 wave periods illustrated in figure 3.

When the root-mean energy ϵ is increased further, the nonlinear modulation retains the same form as in figure 3 except that the modulation period decreases. For $\epsilon > 0.16$ approximately, the nonlinear energy transfer to the higher harmonics causes the time evolution calculations to fail before the nonlinear modulation is established. The SC standing waves follow the same long-time evolution except that the modulation periods are longer. The modulation period for the standing wave SC when $\epsilon = 0.1$ is 4200 wave periods, compared with the 3160 wave periods of figure 3.

It is not possible to calculate the harmonics of the SB and SD standing waves to the same high numerical precision, using the fixed-point method (§3.2), as it is for the SA and SC waves. When the numerical precision is set so that the error $< 10^{-5}$, the fixed-point method remains in the neighbourhood of a solution instead of converging to it. This appears to be a consequence of the weak dependence of the harmonics on their phases compared with the dependence on their amplitudes. The phases are fixed at zero or π for the SA and SC waves, but a similar constraint is not applicable to the SB and SD waves. There is not sufficient numerical precision to obtain meaningful polynomial expansions for the frequency ω and the amplitude a_{42} of the SB and SD waves in terms of the fundamental amplitude a_{11}. However, the precision is sufficient to observe that the frequency for the SB and SD waves is found to follow the same curve, within a difference of less than 10^{-4}, as that for the SA and SC waves over the range $0 < \epsilon < 0.2$. Also, the amplitude ratio a_{42}/a_{11} for the SB and SD waves lies close to that for the SA and SC waves over the range $0 < \epsilon < 0.05$ (4.3*b*), but progressively departs from it at larger ϵ.

When the long-time evolution of the SB and SD waves is calculated at $\epsilon = 0.05$, their harmonic amplitudes stay almost constant over the 10000 wave periods of the calculation, despite the result below (2.22*d*), but like the SA and SC waves at the same value of ϵ, the phase α_{42} of the dominant fourth component relative to the phase α_{11} of the dominant first component drifts from its initial value over the same long time. The SB and SD waves do not evolve into a nonlinear modulation of the harmonics at higher values of ϵ like the SA and SC waves, as illustrated in figure 3. Instead, for $\epsilon = 0.1$, the harmonics remain constant in amplitude and phase for about 3000 wave periods, then the calculation progressively fails because the nonlinear transfer of energy to the higher harmonics causes energy accumulation at the truncation harmonics. The harmonics remain constant for about 200 wave periods at $\epsilon = 0.15$, and only for about 30 wave periods at $\epsilon = 0.2$, before failure of the calculations. The time intervals over which the wave amplitudes remain close to their initial values are of comparable length to those found for the SA and SC waves, indicating that all four types of standing waves are of comparable stability.

4.3. *Standing waves with resonating first and ninth harmonics*

The weakly nonlinear theory predicts that pure standing waves exist for which the first and ninth harmonics interact resonantly with the amplitude ratio (2.16)

$$a_{93}/a_{11} = \tfrac{1}{9}$$

in the present notation (3.8*a*, *b*). The only pure standing waves of this type that have been predicted theoretically and found computationally have the values 0, π for the phase α_{93} relative to the phase α_{11}. These two are denoted by standing waves SNA, SNC respectively. The letter S indicates that, as with the Stokes standing waves, the amplitude a_{11} is dominant, the letter N indicates that the amplitude a_{42} is almost null, and the third letter indicates that the phase α_{93} relative to α_{11} is zero or π for the two solutions respectively.

The fixed-point computational method (§3.2) converges rapidly to the SNA and SNC standing wave solutions with high numerical precision (error $< 10^{-10}$), up to $\epsilon = 0.2$. Like the Stokes standing waves, the time origin may be chosen so that all the Fourier sine coefficients in (3.2*a*, *b*) for the SNA and the SNC waves are zero. The frequency ω and resonant amplitude a_{93}, expanded as polynomials in the fundamental amplitude a_{11} over the range $0 < \epsilon < 0.05$, are found to have the leading terms

$$\omega = 1.000000 - 0.1250a_{11}^2 + \ldots \quad \text{and} \quad a_{93} = 0.11111a_{11} - 1.230a_{11}^3 + \ldots, \quad (4.4a, b)$$

for both the SNA and SNC standing waves. The phase α_{93} (relative to α_{11}) is zero for the SNA waves and π for the SNC waves. This expansion confirms (2.16) and has a similar form to (4.3*b*), with the linear and cubic leading terms arising from the resonant interaction between the first and ninth harmonics. Apart from the maximum near a_{93}, the remaining harmonic amplitudes for the SNA and SNC waves lie close to a Stokes ordering.

The stability of the SNA and SNC standing waves for root-mean energies in the range $0 < \epsilon < 0.2$ is determined by calculating their long-time evolution (§3.3) for up to 10000 wave periods. At $\epsilon = 0.05$, the harmonic amplitudes of both the SNA and SNC waves stay almost constant over the 10000 wave periods, but the phase α_{93} of the dominant ninth component relative to the phase α_{11} of the dominant first component drifts monotonically by more than π over the same long time. Their long-time behaviour at this value of ϵ is almost identical with that of the SA and SC waves.

Unlike the SA and SC waves, a more predictable long-time behaviour occurs when the root-mean energy is increased to $\epsilon = 0.1$. The linear stability analysis (2.21*a–c*) indicates that the standing waves SNA and SNC at this energy are unstable. The time evolution of the SNA wave at $\epsilon = 0.1$ is illustrated in figure 4 starting from the fixed-point standing wave solution, with the only disturbance being the initial numerical error. It can be seen that the standing wave amplitudes remain near their initial values for about 250 wave periods before evolving into nonlinear modulated oscillations. This initial behaviour is consistent with the instability predicted by (2.21*c*).

When the fast time variation of the amplitudes in (3.6*a*, *b*) is decomposed with respect to one modulation period equal to 301 wave periods (effectively a Fourier decomposition into a continuum of frequencies), it is found that the energy in the wave components during the modulated oscillations occurs dominantly in wavebands centred near the *free components* with frequencies $\omega(m) = m^{\frac{1}{2}}, m = 8, 9, 10$. The *bound components* of the sidebands which were dominant in the nonlinear modulated oscillations evolving from the SA and SC waves (§4.2) have energies which are not much greater than the background level here. There are also bound components with

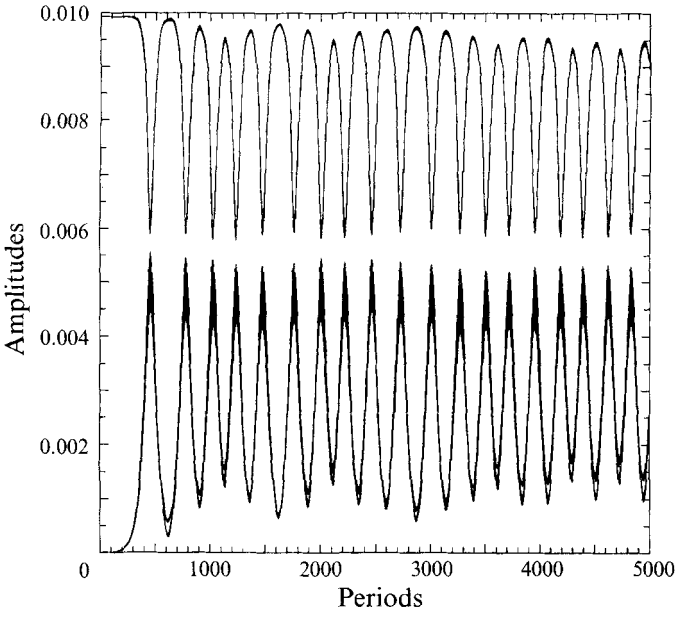

FIGURE 4. The time evolution of the resonant amplitude a_{93} at the top, then in order the two sideband amplitudes a_{83} and a_{103} almost superposed, starting from the standing wave SNA with $\epsilon = 0.1$.

small energies generated by the free components, such as those at wavenumber 9 with frequencies near $\sqrt{8}\pm 1, \sqrt{10}\pm 1$. The fundamental wave component with amplitude a_{11} plays a passive role in the nonlinear modulated oscillations evolving from the SNA and SNC waves, and remains almost constant over the long time illustrated in figure 4. This property is in contrast to the nonlinear modulated oscillations evolving from the SA and SC waves, where it can be seen in figure 3 that the long-time evolution of the amplitudes a_{11} and a_{42} is oscillatory and opposite in phase so that the total energy is conserved.

The total energy in figure 4 decreases by less than 0.1 % over the 5000 wave periods illustrated. It is noted that the nonlinear modulated oscillations evolving from the SNA and SNC waves have a similar structure to those evolving from the sideband instability of the set of nine Stokes standing waves with the same value of ϵ (§4.1, figure 2). When the root-mean energy ϵ is increased further, the nonlinear modulation retains the same form as in figure 4 except that the modulation period decreases. The SNC standing waves follow the same long-time evolution as the SNA waves, with comparable modulation periods.

4.4. *Standing waves with resonating first, fourth and ninth harmonics*

It was shown in §2.3 that the third-order theory not only admits pure standing wave solutions in which resonant interactions occur between the two harmonics with amplitudes a_{11}, a_{42} or with amplitudes a_{11}, a_{93}, but also those in which resonant interactions occur between all three harmonics with amplitudes a_{11}, a_{42}, a_{93}. The theory indicates that these standing waves have the same frequency relation (2.14*a*) and the same amplitude ratio (2.15), (2.16) as the other two waves.

A number of different standing wave solutions of this type have been found by the fixed-point method (§3.2) and their properties investigated by the time evolution method (§3.3). If the known phase relations from the two previous sections are

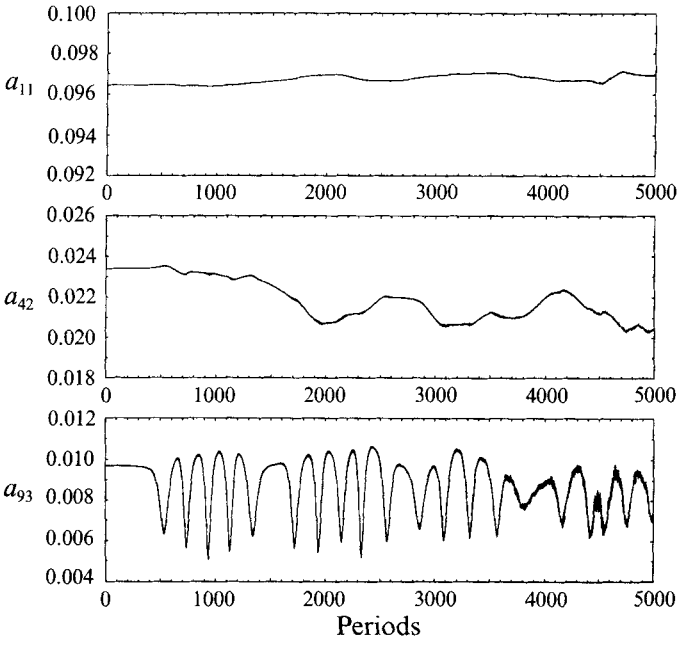

FIGURE 5. The time evolution of the resonant amplitudes a_{11}, a_{42} and a_{93}, starting from the standing wave SAC with $\epsilon = 0.1$.

combined, there are in principle eight different solutions of this type. The phase α_{42} relative to the phase α_{11} (2.20) may be $0, \frac{1}{2}\pi, \pi, \frac{3}{2}\pi$, and the phase α_{93} relative to the phase α_{11} may be $0, \pi$. The solutions are denoted SAA, SAC, SCA, SCC, SBA, SBC, SDA, SDC, with an obvious notation that combines the previous ones. The first four solutions, in which all phase differences are 0, π, have Fourier expansions (3.2*a*, *b*) with no sine terms. The only solution of the last four which has been found with confidence is the wave SBC, and its properties are similar to those of the first four waves.

The properties of the wave SAC are described now, as a representative of the above five standing waves. The fixed-point computational method (§3.2) converges rapidly to the SAC standing wave solutions with high numerical precision (error $< 10^{-10}$). The leading terms of the polynomial expansions for the frequency and the resonant amplitudes of the wave SAC over the range $0 < \epsilon < 0.05$ are

$$\omega = 1.000000 - 0.1250a_{11}^2 + \ldots, \quad a_{42} = 0.25000a_{11} - 0.786a_{11}^3 + \ldots, \quad (4.5a, b)$$

and

$$a_{93} = 0.11111a_{11} - 1.107a_{11}^3 + \ldots. \quad (4.5c)$$

The phase α_{93} (relative to α_{11}) is π for the SAC waves. The two leading terms of the expansion for ω agree with (2.14*a*), and the leading terms of the expansions for a_{42} and a_{93} agree with (2.15) and (2.16) respectively.

The stability of the SAC standing wave for root-mean energies in the range $0 < \epsilon < 0.2$ is determined by calculating their long-time evolution (§3.3). At $\epsilon = 0.05$, the harmonic amplitudes stay almost constant over the 10000 wave periods of the calculation, but the phases α_{42}, α_{93} of the dominant components relative to the phase α_{11} of the first component drift over the same long time.

The long-time evolution when the root-mean energy is increased to $\epsilon = 0.1$ is illustrated in figure 5, starting from the fixed-point standing wave solution with the only disturbance being the initial numerical error. It can be seen that the standing wave

amplitudes remain near their initial values for about 400 wave periods before evolving into nonlinear modulated oscillations. Their subsequent evolution consists of the slow change observed in figure 3 for the amplitudes a_{11} and a_{42}, superposed on the fast modulation observed in figure 4 as the amplitude a_{93} interacts independently with the free components in its sidebands. The root-mean energy ϵ changes by less than 0.1% over the first 3500 wave periods illustrated, and then by about 0.3% over the last 1500 wave periods associated with the change in appearance of the modulation.

When the root-mean energy is increased to $\epsilon = 0.15$, the SAC standing wave amplitudes remain near their initial values for about 100 wave periods. They then begin nonlinear modulated oscillations similar to those in figure 5 except that the modulation periods are smaller. These terminate after a further 250 wave periods when the nonlinear energy transfer to the higher harmonics causes the time evolution calculations to fail.

4.5. *Standing waves with resonating fourth and ninth harmonics*

The third-order theory in §2.3 not only admits pure standing wave solutions in which resonant interactions occur between the two harmonics with amplitudes a_{11}, a_{42} or with amplitudes a_{11}, a_{93}, but also those in which resonant interactions occur between the two harmonics with amplitudes a_{42}, a_{93} while the fundamental amplitude a_{11} remains much smaller. The theory (2.17*b*) indicates that these standing waves have an amplitude ratio

$$a_{93}/a_{42} = \tfrac{4}{9}.$$

The standing wave solutions of this type have been found by the fixed-point method (§3.2) and their properties investigated by the time evolution method (§3.3). The argument based on phases advanced in the previous section indicates that there are in principle eight different solutions of this type. The only two solutions of this type that have been found with any confidence are denoted by NAC and NCC, where N indicates that the amplitude a_{11} is almost null, the second letter indicates that the phase α_{42} relative to α_{11} is zero or π in the two solutions, and the third letter indicates that the phase α_{93} relative to α_{11} is π for both solutions. Although $a_{11} \ll a_{42}$ for small ϵ(< 0.05), a_{11} increases as ϵ increases, becoming comparable with a_{42} at about $\epsilon = 0.1$.

The properties of the wave NAC are described now, as a representative of both standing waves of this type. The fixed-point computational method (§3.2) converges rapidly to the NAC standing wave solutions with high numerical precision (error $< 10^{-10}$). The leading terms of the polynomial expansions with respect to a_{42} for the frequency ω and for the amplitude a_{93} over the range $0 < \epsilon < 0.05$ are

$$\omega = 1.000000 - 2.072a_{42}^2 + \ldots, \quad a_{93} = 0.4445a_{42} + \ldots. \tag{4.6a, b}$$

The phase α_{93} (relative to α_{11}) is π for the NAC waves. Better agreement with the weakly nonlinear theory is found with the corresponding relations at $\epsilon = 0.001$, which are

$$\omega = 1.000000 - 2.0000a_{42}^2, \quad a_{93} = 0.44446a_{42}. \tag{4.6c, d}$$

Equation (4.6*c*) agrees with (2.17*a*) and (4.6*d*) agrees with (2.17*b*).

The stability of the NAC standing wave for root-mean energies in the range $0 < \epsilon < 0.1$ is determined by calculating their long-time evolution (§3.3). Because the amplitude a_{11} is much smaller than previously, it is necessary to choose the root-mean energy ϵ to be smaller than in the previous examples so that the other resonant amplitudes have values comparable with those chosen previously. For this reason, the value chosen for the long-time evolution illustrated in figure 6 is only $\epsilon = 0.05$. It can

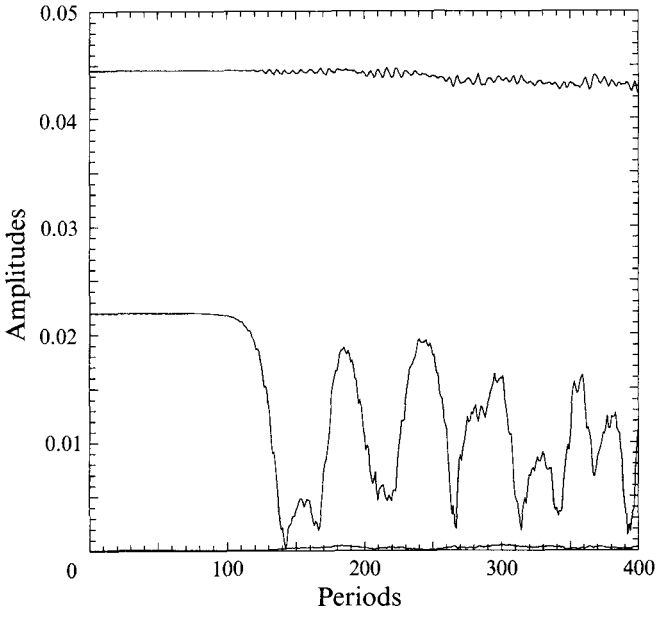

FIGURE 6. The time evolution of the amplitudes a_{42} at the top of the figure, a_{93} next, and a_{11} (which is so close to zero that it is barely visible at the bottom of the figure), starting from the standing wave NAC with $\epsilon = 0.05$.

be seen that the standing wave amplitudes remain near their initial values for about 100 wave periods before evolving into nonlinear modulated oscillations. Their subsequent evolution is similar to that illustrated in figure 4. The amplitudes a_{11} and a_{42} are almost passive, while the amplitude a_{93} interacts independently with the free components in its sidebands. The root-mean energy ϵ changes by about 0.8 % over the 400 wave periods illustrated, but remains constant over the initial 100 wave periods while the standing wave stays near its initial amplitudes.

When the root-mean energy is increased to $\epsilon = 0.1$, the NAC standing wave amplitudes remain near their initial values for about 20 wave periods before the nonlinear energy transfer to the higher harmonics causes the time evolution calculations to fail.

5. Summary and discussion

The Stokes standing wave S was the only known pure standing wave until Agnon *et al.* (1992) found four new waves, denoted by us SA, SB, SC, and SD. In the present paper we have studied these four new waves, and presented nine additional different forms of pure standing waves namely SNA, SNC; SAA, SAC, SCA, SCC, SBC; NAC, NCC. This is not expected to be a complete list, and we discuss the rather peculiar combination SAAA... below.

The existence of the above new standing waves is in clear contrast to a remark by Schwartz & Whitney (1981, p. 168), in a footnote. Their resonance-suppression requirement removes harmonics which cause secular terms. The secular terms arise from the approximation of nonlinear resonance by linear resonance in the equations governing the small-amplitude expansions. The removal of the harmonics is a denial of the existence of the resonant maxima which are the distinguishing feature of the above new standing waves.

The agreement between our two approaches: (i) weakly nonlinear theory, and (ii) fully nonlinear computation, ensures that these solutions are genuine. We have shown that the solutions are not less stable than the original Stokes standing waves, and thus deserve attention in future investigations and applications. For example, the Fourier amplitudes of the standing wave SA in figure 3 remain close to their initial values for over 1000 wave periods before they evolve into a slow modulation. The sideband modulation in figures 2 and 4 is of special interest because it exhibits the same form of cyclic recurrence as the Stokes progressive waves. The question of the conditions for the generation of the new standing waves in a more realistic forced and damped system is an important objective for a future study.

Most of the examples presented in the figures remain almost unchanged over initial intervals which are typically hundreds of wave periods. The question arises as to whether an instability such as that in figure 3 for an inviscid fluid is only of academic interest for real fluids. The theory for oscillating boundary layers may be adapted to show that the half-life for a Stokes standing wave in a deep square tank of side l containing a fluid of kinematic viscosity ν is N wave periods approximately, where

$$N = 0.075 l^{\frac{3}{4}} g^{\frac{1}{4}} / \nu^{\frac{1}{2}}. \tag{5.1}$$

For water at 20 °C, $N = 133$ when $l = 1$ m, but $N = 4200$ when $l = 100$ m.

The presence of significant higher harmonics in the new standing waves becomes of greater importance for the water surface slope and acceleration. This is demonstrated with an exaggerated extension (ignoring surface tension and viscosity) to a possible wave SAAA.... The free surface of this 'wave' is

$$\eta = a_1 \sum_{n=1}^{\infty} \frac{1}{n^2} \cos(n^2 kx) \cos[n(gk)^{\frac{1}{2}} t], \tag{5.2}$$

obtained as a generalization of combining (2.9*a*) with (2.15), (2.16). The energy of this 'wave' is approximately

$$\tfrac{1}{4}\rho g a_1^2 \sum_{n=1}^{\infty} \frac{1}{n^4} = \tfrac{1}{4}\rho g a_1^2 \frac{\pi^4}{90} = 1.082\,(\tfrac{1}{4}\rho g a_1^2), \tag{5.3}$$

which is only about 8% greater than the energy of the fundamental harmonic given in parentheses. However, the vertical acceleration of the free surface ($\sim \partial^2\eta/\partial t^2$) diverges almost everywhere. The geometry of η at any given time is rather complicated. At $t = 0$, it takes the form of Riemann's continuous but non-differentiable function (Mandelbrot 1982)

$$R = \sum_{n=1}^{\infty} \frac{1}{n^2} \cos(n^2 \zeta), \tag{5.4}$$

which can be shown to be a multifractal function with a dimension ≈ 1.19.

M.S. acknowledges the support of the US Office of Naval Research, Contract N00014-91-J-1449, and the award of an Erskine Visiting Fellowship at the University of Canterbury. He is grateful to the Head and staff of the Mathematics Department, University of Canterbury, for their hospitality.

REFERENCES

AGNON, Y., DOLD, J. W., GLOZMAN, M., MILMAN, T. & STIASSNIE, M. 1992 New standing water–wave solutions. In *Order and Chaos in Standing Waves, Second Scientific Report, Coastal and Marine Engineering Research Institute, Technion, Haifa, Israel.* P.N. 305/92.

AMICK, C. J. & TOLAND, J. F. 1987 The semi-analytic theory of standing waves. *Proc. R. Soc. Lond.* A **411**, 123–137.

BRYANT, P. J. 1985 Doubly periodic progressive permanent waves in deep water. *J. Fluid Mech.* **161**, 27–42.

GLOZMAN, M., AGNON, Y. & STIASSNIE, M. 1993 High order formation of the water–wave problem. *Physica* D **66**, 347–367.

LAKE, B. M., YUEN, H. C., RUNGALDIER, H. & FERGUSON, W. E. 1977 Nonlinear deep-water waves: theory and experiment. Part 2. Evolution of a continuous wave train. *J. Fluid Mech.* **83**, 49–74.

MANDELBROT, B. 1982 *The Fractal Geometry of Nature.* Freeman.

MERCER, G. N. & ROBERTS, A. J. 1992 Standing waves in deep water: Their stability and extreme form. *Phys. Fluids* A **4**, 259–269.

OKAMURA, M. 1984 Instabilities of weakly nonlinear standing gravity waves. *J. Phys. Soc. Japan* **53**, 3788–3796.

PENNEY, W. G. & PRICE, A. T. 1952 Finite periodic stationary gravity waves in a perfect liquid. *Phil. Trans. R. Soc. Lond.* A **244**, 254–284.

RAYLEIGH, LORD 1915 Deep water waves, progressive or stationary, to the third order of approximation. *Proc. R. Soc. Lond.* A **91**, 345–353.

ROTTMAN, J. W. 1982 Steep standing waves at a fluid interface. *J. Fluid Mech.* **124**, 283–306.

SAFFMAN, P. G. & YUEN, H. C. 1979 A note on numerical computations of large amplitude standing waves. *J. Fluid Mech.* **95**, 707–715.

SCHWARTZ, L. W. & WHITNEY, A. K. 1981 A semi-analytic solution for nonlinear standing waves in deep water. *J. Fluid Mech.* **107**, 147–171.

STIASSNIE, M. & SHEMER, L. 1984 On modifications of the Zakharov equation for surface gravity waves. *J. Fluid Mech.* **143**, 47–67.

TAYLOR, G. I. 1953 An experimental study of standing waves. *Proc. R. Soc. Lond.* A **218**, 44–59.

WEST, B. J. 1981 *Deep Water Gravity Waves.* Lecture Notes in Physics, vol. 146. Springer.

ZAKHAROV, V. E. 1968 Stability of periodic waves of finite amplitude on the surface of a deep fluid. *J. Appl. Mech. Tech. Phys.* **2**, 190–194.